Respuestas
Journal of Engineering Sciences
RESPUESTAS

Original Article https://doi.org/10.22463/0122820X.2557

# Induction motor speed control in a DSP-based low-THD multi-level converter

## Control de velocidad del motor de inducción en un convertidor multinivel de bajo THD basado en DSP

Edison Andrés Caicedo-Peñaranda[1*], Henry Alfonso Sepúlveda-Pacagui[2], Luis David Pabón Fernández[3], Aldo Pardo-García[4*], Jorge Luis Díaz-Rodríguez[5]

[1]*Magíster en controles industriales, eacaicedop@gmail.com, Orcid: 0000-0003-4557-1061, Universidad de Pamplona, Pamplona, Colombia.*
[2]*Ingeniero eléctrico, sepu08@hotmail.com, Orcid: 0000-0002-1845-6503, Universidad de Pamplona, Pamplona, Colombia.*
[3]*Magíster en controles industriales, davidpabon@hotmail.es, Orcid: 0000-0003-1788-4781, Universidad de Pamplona, Pamplona, Colombia.*
[4*]*Posdoctor en ingeniería eléctrica, apardo13@hotmail.com, Orcid: 0000-0003-2040-9420, Universidad de Pamplona, Pamplona, Colombia.*
[5]*Magíster en automática, jdiazcu@gmail.com, Orcid: 0000-0001-7661-8665, Universidad de Pamplona, Pamplona, Colombia.*

**How to cite:** E.A. Caicedo-Peñaranda, H.A. Sepúlveda-Pacagui, L.D. Pabón-Fernández, A. Pardo-García, J.L. Díaz-Rodríguez "Induction motor speed control in a DSP-based low-THD multi-level converter". *Respuestas,* vol. 25, no. 1, pp. 159-167, 2020.

Received on July 30, 2019; Approved on November 26, 2019

**ABSTRACT**

This paper presents the development of an algorithm for speed control for the induction motor using the TMS320F28069M microcontroller, the algorithms were performed based on the operating limits of the scalar control technique and the characteristics of the DSP. The control technique together with the optimization algorithm used will provide the modulations with optimization of the harmonic content, based on the method of frequency variation adopting a multi-level converter, which receives the control signals from the device's GPIOs acting as the final element control loop proposed. The adopted multilevel converter converts the voltage coming from the DC BUS to a quasi-sinusoidal AC voltage thanks to the steps outlined above, providing the power supply to the induction motor that intrinsically carries the scalar control technique.

**Keywords:**

Harmonic Distortion, Power Inverter, Optimization, speed control, embedded systems.

**RESUMEN**

Este artículo presenta el desarrollo de un algoritmo para el control de velocidad del motor de inducción utilizando el microcontrolador TMS320F28069M, los algoritmos se realizaron en función de los límites operativos de la técnica de control escalar y las características del DSP. La técnica de control junto con el algoritmo de optimización utilizado proporcionará las modulaciones con la optimización del contenido armónico, basado en el método de variación de frecuencia que adopta un convertidor multinivel, que recibe las señales de control de los GPIO del dispositivo que actúan como control del elemento final propuesto. El convertidor multinivel adoptado convierte el voltaje proveniente del BUS DC en un voltaje de CA casi sinusoidal gracias a los pasos descritos anteriormente, proporcionando la fuente de alimentación al motor de inducción que lleva intrínsecamente la técnica de control escalar.

**Palabras clave:**

Dimensión gerencial, habilidades gerenciales, liderazgo, perfil gerencial, toma de decisiones.

## Introduction

The microcontroller of the family Piccolo™ C2000 [1], where the kit LAUNCHXL-28069M is of low cost and high efficiency useful for control applications [2], where the three-phase induction motor is widely used in the industry under speed conditions specified by the application that requires a power converter [3], where these have had significant advances [4], [5], therefore the present work employs a multilevel H-bridge cascade converter of common source with optimized harmonic content embedded in the DSP [6].

By using control techniques in the TMS320F28069M great advantages are obtained as far as the input data processing since each data must be multiplied, added and in addition to that transformed according to complex formulas, this is obtained since they are designed for tasks of high repetitive and numerically intense benefits, the great speeds that offer these devices to us allow that the treatment is made of very efficient form, in addition that they allow us to have control of many variables of the

***Corresponding author.**
E-mail Address: *eacaicedop@gmail.com* (Edison Andrés Caicedo-Peñaranda)

system to controlled limited only by the characteristics of DSP used [7] and the advantages of low cost [8], favoring even projects with low budget, because regulation and improvement of equipment delays the execution of works in sectors such as agribusiness [9].

### *Control methodology*

The induction motor is controlled by a V/F law, with modulations obtained by a multi-target genetic algorithm [10], where the obtained modulations are sent to the TMS320F28069M card which is in charge of sending the control signals to the converter semiconductors, acquire data for further processing and control for the three-phase induction machine [11], the overall system is designed to minimize the harmonic content of the input current, to precisely regulate the DC bus [12] the advanced control approach thought for the future [13] - [15].

The speed of the induction motor is measured by a DC motor Figure 1, which is a permanent magnet motor that generates DC voltage depending on the speed at which its rotor rotates, acting as a transducer by converting speed to a voltage value.

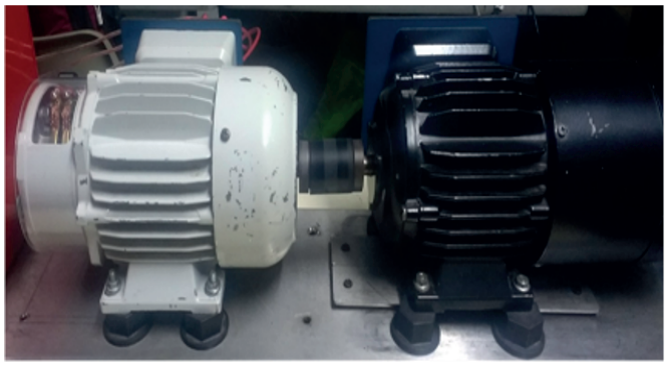

**Figure 1.** Induction motor speed measurement.

The voltage signal is filtered and conditioned to acceptable values from analogue DSP inputs, this was done with the integrated TL074CN [16].

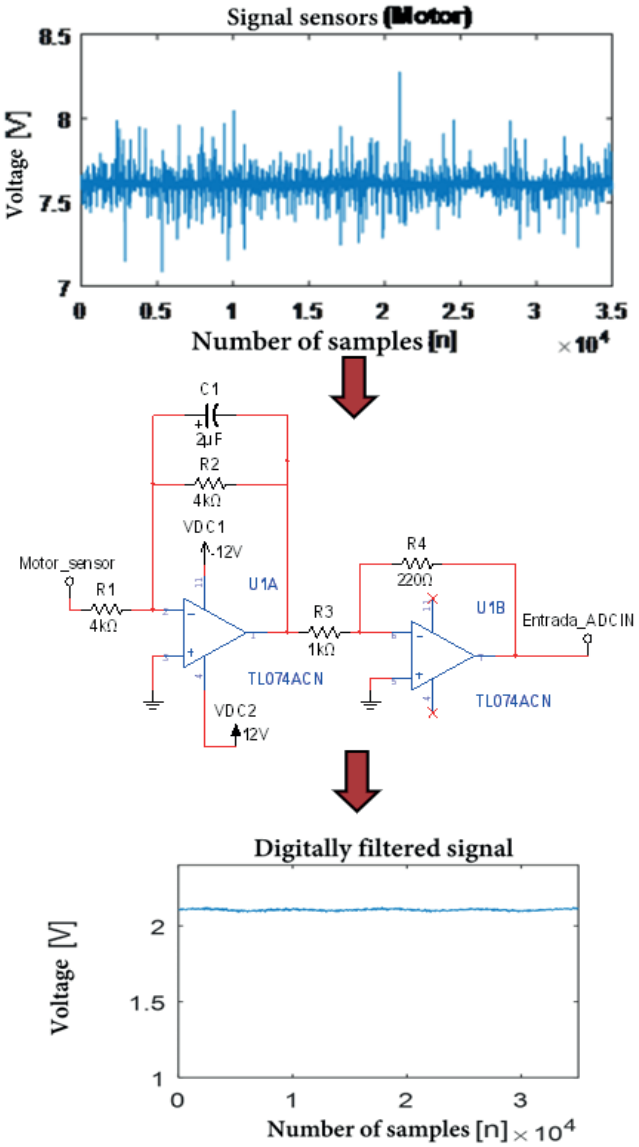


**Figure 2.** Speed signal.

### *Implementation of the control technique*

The multilevel inverter topology which was adopted as can be seen in Figure 3 is an asymmetrical common source cascade H-bridge converter with a 1:3 ratio and two 2 stages in each phase providing 9 levels of voltage and 15 levels in the line voltage which was described and implemented in works [17].

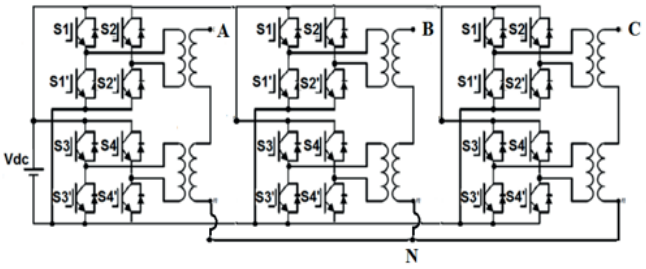


**Figure 3.** Topology of the adopted converter [17].

### *Optimization Algorithm*

The genetic algorithm in equations 1 and 2 described in works [10] and [17] and in accordance with the IEEE 519 standard of 1992 [18], defines the total harmonic distortion calculated up to the 50th harmonic where the h1 harmonic is the fundamental component and $h_n$ the peak of the n harmonic:

$$THD = \frac{\sqrt{\sum_{n=2}^{50}\left\{\frac{1}{n}\left[\sum_{i=1}^{4}\sum_{j=1}^{L_i}(-1)^{j-1}\cos n\alpha_{ij}\right]\right\}^2}}{\left[\sum_{i=1}^{4}\sum_{j=1}^{L_i}(-1)^{j-1}\cos 1\alpha_{ij}\right]}\cdot 100 \qquad (1)$$

Where n takes odd values different from three because the harmonics multiple of 3 are suppressed in the connection of the transformers, that is 5, 7, 11, 13, 17, ... and Li are the components of the vector $L$= [a b c d] (at level 1, b level 2, c level 3 and level 4); Para, the rms value can be defined [10].

$$V_{line_{RMS}} = \sqrt{\sum_{\substack{n=1 \\ n=5,7,\cdots,}}^{50}\frac{\left\{\frac{4\sqrt{3}V_{CD}}{\pi n}\left[\sum_{i=1}^{4}\sum_{j=1}^{L_i}(-1)^{j-1}\cos n\alpha_{ij}\right]\right\}^2}{2}} \qquad (2)$$

different multiples of three

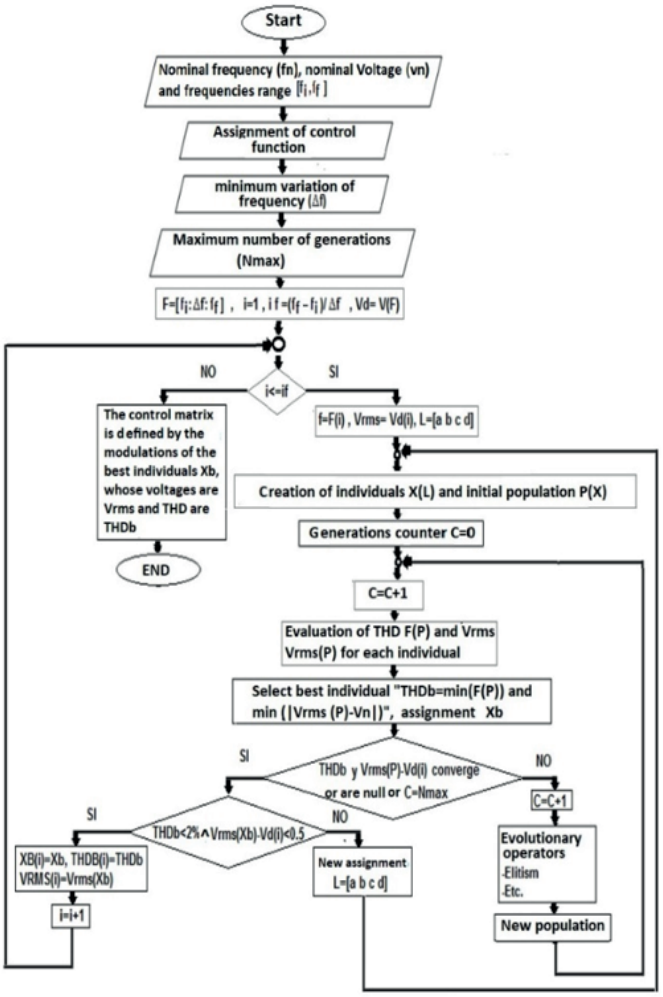


**Figure 4.** Multi-target genetic algorithm [10].

### *Results of the optimization algorithm*

With the machine's nominal voltage assignment at 220 *Vrms*, the nominal frequency 50 Hz, the frequency range will be [45 *Hz*, 55 *Hz*] with steps of Δf=1 *Hz*, the Vboost level is set at 30 *Vrms* line. With these data the algorithm was run in Matlab and the activation angles of 11 modulations with low harmonic content and RMS values following the law V vs f were obtained with the previous data [10]. Giving the exact switching angles or state changes of the GPIO pins of the card described for the frequency range pre-set in the genetic algorithm was obtained as a matrix [10] which has switching angles and positions.

### *Speed control technique algorithm in TMS320F28069M*

In this algorithm the respective code controlling the

control technique described above is processed so that each modulation generated by control pins on the card corresponds to its respective frequency and also each position of the time vector corresponds to its respective state of the state vector. The main code includes, in addition to the proposed algorithms, header files, source files, libraries, specific development libraries and other configurations and/or routing performed [19]; this is exemplified in the diagram in figure 6 all programming was done in code composer studio in CCS [20].

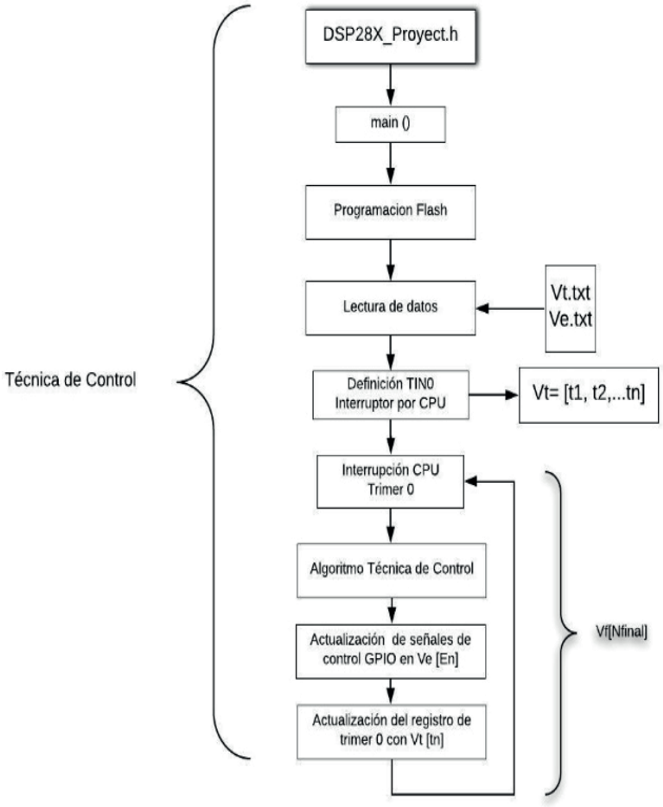


**Figure 6.** Speed control technique algorithm.

In the algorithm in the initial stage the state vectors "Ve[]" and switching time vectors "Vt[]" previously found with the multi-target genetic algorithm are loaded into the DSP. A CPU interruption caused by timer 0 [21] is defined where the time vector values and states are loaded generating an optimized modulation [22] in accordance with the data loaded into the DSP.

### *Overview of the speed control algorithm of the induction motor in tms320f28069m*

The control is based on the principle of the loop shown in figure 7, where the value of the rotor speed depends on a motor coupled to the shaft that works as a generator producing a DC voltage level that is proportional to the speed in an instant of time.

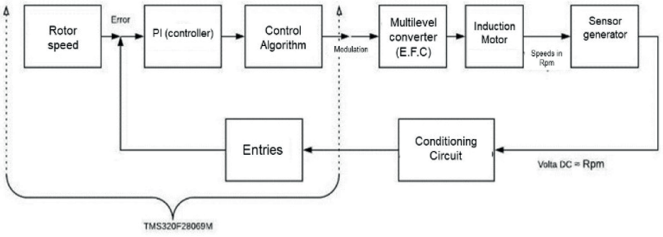


**Figure 7.** System Control Loop

The general algorithm of the induction motor speed control comprises the inclusion of each of the stages proposed above in the same algorithm. With the correct implementation of the control technique at code level, the most general control algorithm is created, comprising a PI controller [22], together with its feedback input provided by an analogue port; the simplified description of the procedure for the development of the general control algorithm is exemplified in Figure 8.

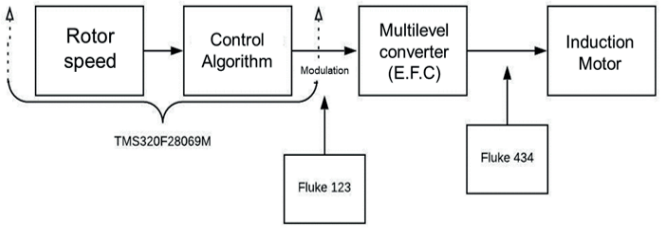


**Figure 8.** General algorithm diagram.

### *Performance testing and validation*

Figure 9 shows the assembly carried out in order to validate the open-loop system outputs in block diagram mode.

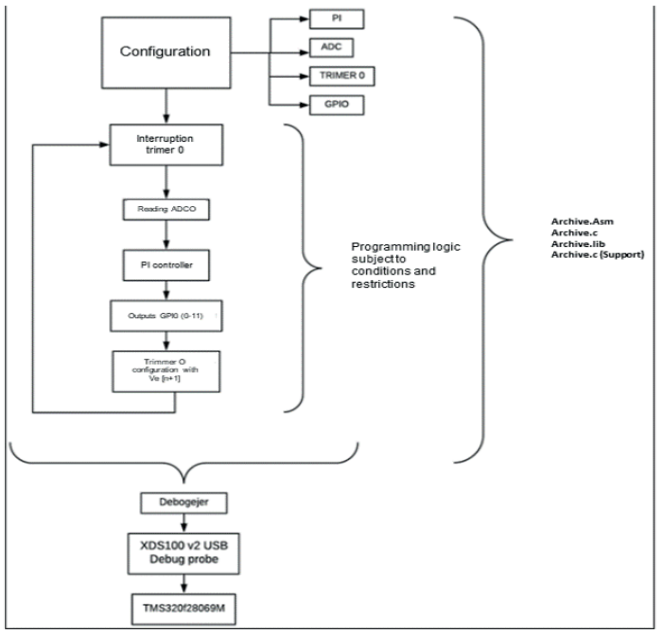


**Figure 9.** Mounted system.

Figure 10 shows the system adopting the multilevel inverter [17].

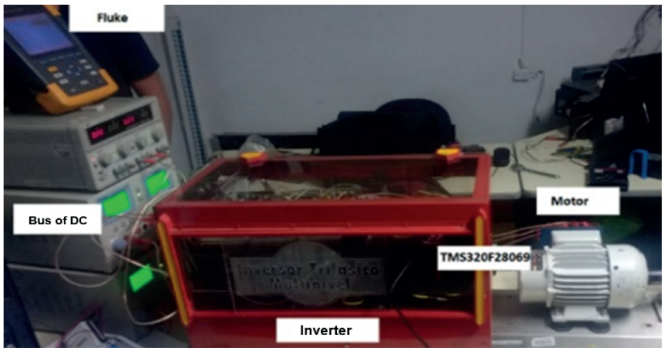


**Figure 10.** Assembly of the proposed scheme.

### *Optimized modulations.*

Figure 11, shows the measurements recorded with the Fluke 123 instrument in 45Hz, 50Hz and 55Hz of the established control, in the measurement only the sum of all the modulation times of a GPIO was taken.

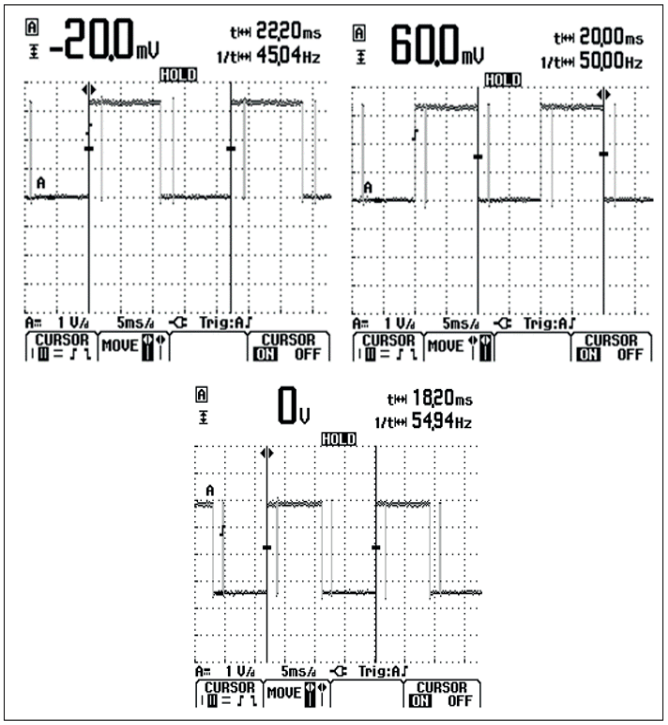


**Figure 11.** Low frequency modulations.

### *Voltage and THD waveforms*

The waveforms generated by the switching of the Mosfet semiconductors as a whole by the DC bus of the three-phase power inverter have a low THD percentage figure 12, the quasi-sinusoidal waveforms obtained validate both the programming logic and the correct application of the scalar law of the motor that is why the Fluke 434 Network Analyzer is used which conforms to the IEC 61000-4-7 standard.


Respuestas, 25 (1), pp. 159-167, 2020, ISSN 0122-820X - E ISSN: 2422-5053

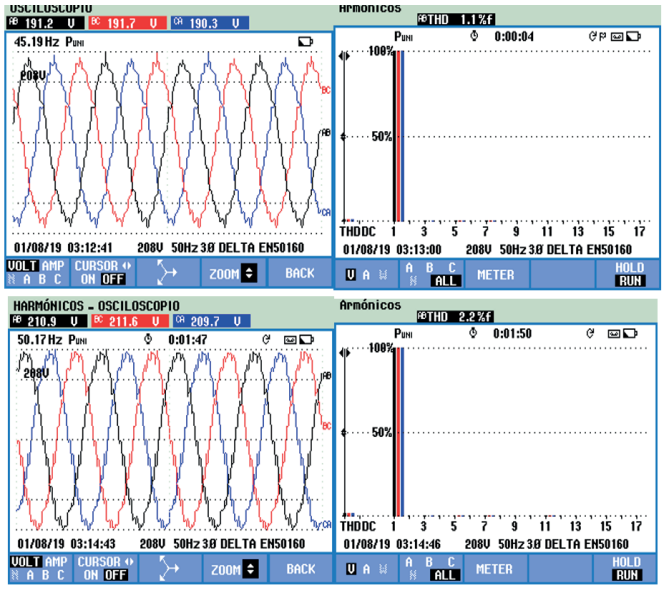


**Figure 12.** Waveforms for line voltage and THD.

With the data loaded in the DSP obtained from the genetic algorithm, the following table is constructed, which contains the data recorded with the measuring instruments recorded at the input of the induction motor such as THD, frequency, line voltage and speed in revolutions per minute.

**Table I.** Electrical variables

| Fn | VL | %THD | Rpm |
|---|---|---|---|
| 45,19 | 190 | 1,1 | 1320 |
| 45,92 | 194 | 1,2 | 1344 |
| 46,97 | 198 | 1,2 | 1374 |
| 48,02 | 202 | 1,2 | 1407 |
| 49,07 | 205 | 1,2 | 1437 |
| 50,17 | 210 | 2,2 | 1471 |
| 51,12 | 211 | 2,1 | 1499 |
| 52,06 | 211 | 2 | 1526 |
| 53 | 212 | 2 | 1553 |
| 53,94 | 213 | 2 | 1581 |
| 54,87 | 213 | 2 | 1609 |

Evidencing the existence of the V/F law in the multilevel converter with low harmonic content measured in practice, building from figure 13 where it denotes the frequency range where the induction machine works.

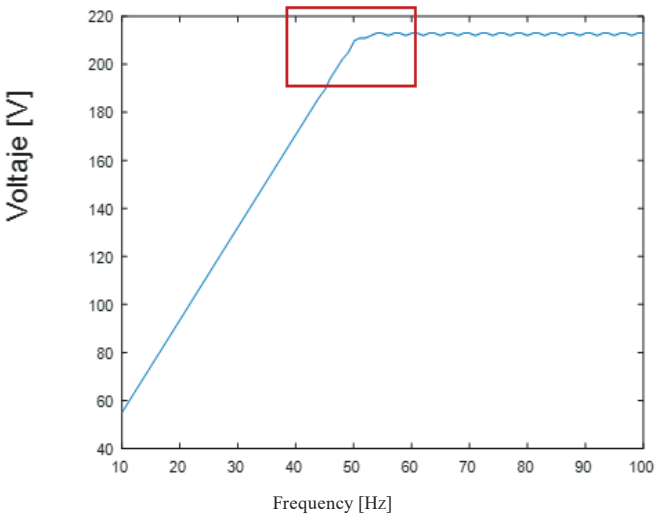


**Figure 13.** Scalar control curve.

## *PI controller*

For the calculation of the parameters of the implemented controller it was tuned in Matlab, starting from the transfer function obtained from the complete identification of the system in open loop figure 14; where the TMS320F28069M controls the multilevel converter according to the stages previously stated together with the speed sensor coupled to the rotor shaft, the data is acquired with a DAQ which processes the data and sends it to a computer.

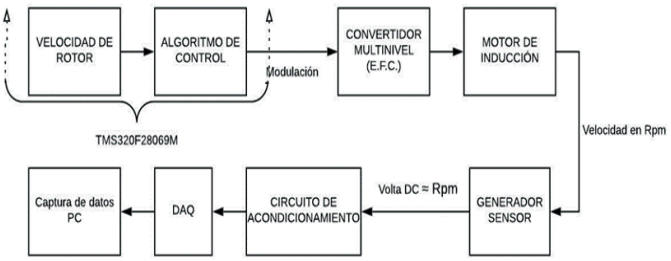


**Figure 14.** Assembly diagram.

With Matlab's system identification tool IDENT we can obtain a model of our plant's behavior from some input variables as shown in figure 15.

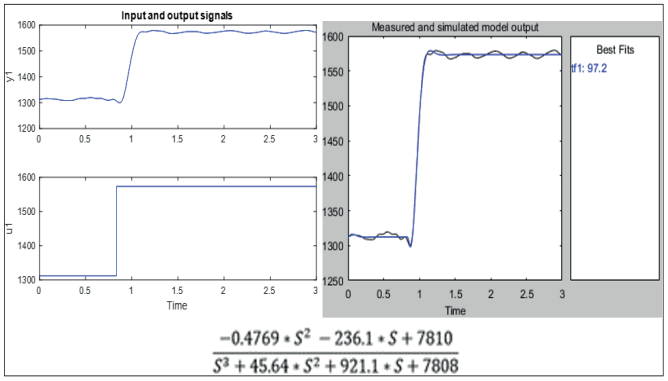


**Figure 15.** System modeling.

A PI controller is simulated and tuned in Matlab according to the plant model obtained previously in figure 16 presents the results obtained.

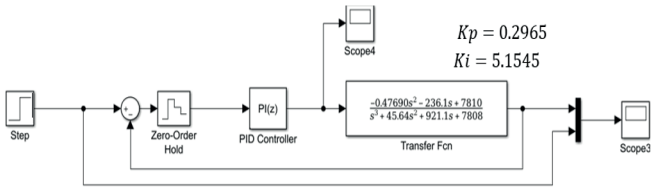


**Figure 16.** System simulation.

### *Operation of the entire closed-loop speed control system*

To carry out the control it was necessary to monitor the important variables in the developed prototype as the reading of the speed sensor, the response of the controller and the error of the control loop, in the figure 17 is appreciated the general assembly of the speed control system.

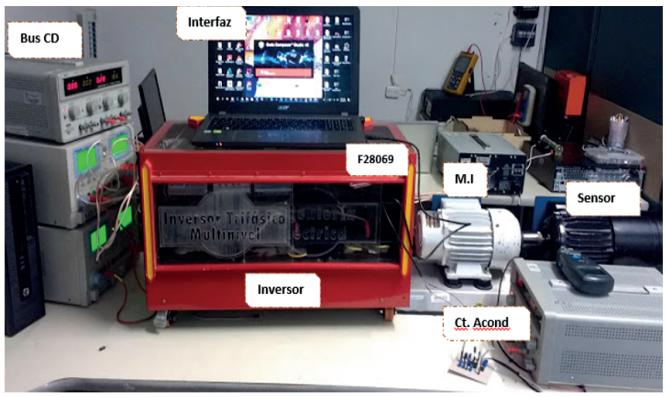


**Figure 17.** Planned assembly.

From an interface, the variables described above are monitored and the controller's rk setpoint is controlled, from which information can be obtained in real time, a prototype of the interface is presented in Figure 18, where the behavior of the proposed control system was monitored.

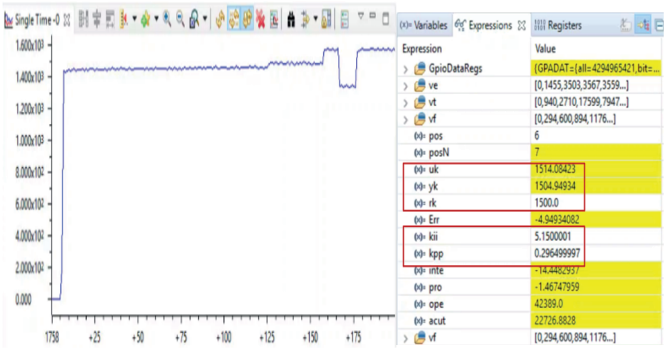


**Figure 18.** Interface.

Through the monitoring interface proposed, a target speed of 1500 Rpm is established, in figure 19 a screenshot of the interface can be seen where rk presents the set point uk response of the e yk controller.

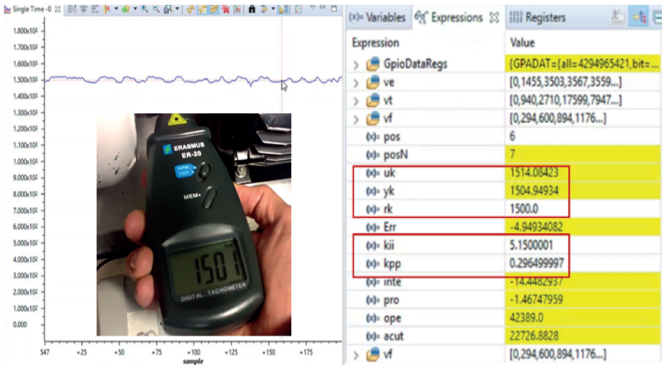


**Figure 19.** Gear change.

Figure 20 shows the modulation change made by the controller in order to reach 1470 *Rpm*. Through the proposed monitoring interface, it is visualized how the different control loops change as yk and rk remain in a relative equilibrium point corroborating that the control system works.


Respuestas, 25 (1), pp. 159-167, 2020, ISSN 0122-820X - E ISSN: 2422-5053

**Figure 20.** Gear change.

## Conclusions

The proposed control adds a low harmonic distortion and properly used the development board LAUNCHXL-F28069M which has excellent performance and low cost. To carry out developments in the CODE COMPOSER STUDIO software, it is necessary to have knowledge about microcontroller architecture, its organization in the different register banks, since this is the main characteristic of this type of programming specifically focused on the TMS320F28060 based on bit field structures, which optimize the memory and also allows any development, especially the one described in this project, to have complete management in execution times. The methodology adopted to find the time vectors and states of the control signals is developed, based and described in a large number of scientific articles specified in references which, together with the F28069M card, improve the power quality in the applied control by decreasing the %THD as well as allowing the developed controller to work in a correct way in conjunction with all phases of development.

The PI controller proposed and developed in CCS language was a correct choice since having only 2 response loops in its block diagram reduced its duration in terms of execution times and program memory overload, optimizing and adapting to the other proposed stages within the card.

## References


[1] Texas Instruments Incorporated, “C2000TM PiccoloTM 32-bit MCU Family”, Dallas, Texas, 2010.

[2] E. Quintero-Manriquez, E. N. Sanchez, R. G. Harley, S. Li and R. A. Felix, "Neural Inverse Optimal Control Implementation for Induction Motors via Rapid Control Prototyping", *IEEE Transactions on Power Electronics*, vol. 34, no. 6, pp. 5981-5992, 2019. doi: 10.1109/TPEL.2018.2870159.

[3] Bermeo, WL, Jr, AB de Souza, Fernández T, Honorio D, Nogueira dos Reis L and Barreto L. “Control modo deslizante aplicado en la malla de corriente para una aplicación de una base-DSP para el control de posición de un motor de inducción de jaula de ardilla”, *Revista Tecnologías de Avanzada*, ISSN: 1692-7257, 2017.

[4] J. A. Araque, J. Rodríguez and A. Guerrero, “Optimización por recocido simulado de un convertidor multinivel monofásico con modulación PWM sinusoidal de múltiple portadora”, *Revista Tecnologías de Avanzada*, ISSN: 1692-7257, 2017.

[5] J. L. Diaz-Rodriguez, L. D. Pabón-Fernández, E. A. Caicedo-Peñaranda and A. Pardo-Garcia, “A Genetic Optimized Cascade Multilevel Converter for Power Analysis”, *Applied Computer Sciences in Engineering*, pp. 123-137, 2016.

[6] K. Preethi, G. Anil and E. Vani, “Speed Control of Induction Motor Using Eleven Levels Multilevel Inverter”, *International Journal of Electrical and Computer Ingeniería*, no. 5, pp. 15–20, 2013.

[7] Texas Instruments Incorporated, “TMS320C28x CPU and Instruction Set Reference Guide”, 2015.

[8] J. Pérez and J. Castro, “LRS1: un robot social de bajo costo para la asignatura “Programación 1” ”, *Revista Tecnologías de Avanzada*, ISSN: 1692-7257, 2018.

[9] A. Bohórquez-Niño, “Microturbina pelton,

una solución real de energía para zonas no interconectadas (ZNI)", *Revista Colombiana de Tecnologías de Avanzadas*, vol. 1, no. 31, pp. 72-76, 2018.

[10] J. L. Diaz-Rodriguez, L. D. Pabon-Fernandez and E. A. Caicedo-Peñaranda, "Multiobjective Genetic Algorithm to Minimize the THD in Cascaded Multilevel Converters with V/F Control", *Applied Computer Sciences in Engineering*, pp. 456-468, 2017.

[11] R. F. Bastos, G. H. Fuzato, C. R. Aguiar, R. V. A. Neves and R. Q. Machado, "Model, design and implementation of a low-cost HIL for power converter and microgrid emulation using DSP", *IET Power Electronics*, vol. 12, no. 14, pp. 3833-3841, 2019. doi: 10.1049/iet-pel.2019.0302.

[12] B. Larimore, "HVAC Dual-AC Motor Control with Active PFC Implementation Using Piccolo TM MCUs", 2010.

[13] J. Castellanos, R. Alvarado and S. Aranguren-Zambrano "Diseño de Estrategia de Control Avanzado para Sistema de Celdas de Flotación en el Tratamiento de aguas de Producción de Petróleo y Gas", Revista Tecnologías de Avanzada, ISSN: 1692-7257, 2015.

[14] A. Pardo-García and L. Castellanos-González, "Automatización de Ambientes en Invernaderos Simulando Escenarios Futuros", *Revista Colombiana de Tecnologías de Avanzada*, ISSN: 1692-7257, vol. 1, no. 29, 2017.

[15] O. Suarez, C. Vega, E. Sánchez, A. González, O. Rodríguez-Jorge and A. Pardo-García, "Degradación anormal de p53 e inducción de apoptosis en la red p53-mdm2 usando la estrategia de control tipo pin", *Revista Tecnologías de Avanzada*, ISSN: 1692-7257, 2018.

[16] Texas Instruments Incorporated, "TMS320x2806x Piccolo Technical Reference Manual", Dallas, Texas, 2017.

[17] E. Peñaranda, J. Díaz and L. Pabón, "Sensorless control of an induction motor with common source multilevel converter", *WSEAS Transactions on Power Systems*, pp. 1-2, 2018.

[18] IEEE, "519-1992 IEEE Recommended Practices and Requirements for Harmonic Control in Electrical Power Systems", *IEEE Std*, 1992.

[19] Texas, 2014. T. I. Incorporated, "C2000 Digital Control Library", no. november, pp. 1–32, 2017.

[20] Texas Instruments Incorporated, "Code Composer StudioTM v8 Integrated Development Environment (IDE) for Embedded Processors", Dallas, 2019.